

Received 25 July 2018; revised 23 August 2018; accepted 18 September 2018. Date of publication 20 September 2018; date of current version 1 October 2018.  
The review of this paper was arranged by Editor S. Reggiani.

Digital Object Identifier 10.1109/JEDS.2018.2871505

# Role of Shape Factor in Forming Surface Electric Field Basin in RESURF Lateral Power Devices and its Optimization Design

JUN ZHANG<sup>1,2</sup> (Member, IEEE), YU-FENG GUO<sup>1,2</sup> (Member, IEEE),  
AND DAVID Z. PAN<sup>1,2,3</sup> (Fellow, IEEE)

<sup>1</sup> College of Electronic Science and Engineering, Nanjing University of Posts and Telecommunications, Nanjing 210003, China

<sup>2</sup> National and Local Joint Engineering Laboratory for RF Integration and Micro-Packaging Technologies, Nanjing University of Posts and Telecommunications, Nanjing 210003, China

<sup>3</sup> Department of Electrical and Computer Engineering, University of Texas at Austin, Austin, TX 78712, USA

CORRESPONDING AUTHORS: J. ZHANG AND Y.-F. GUO (e-mail: bravaisxx@163.com; yfguo@njupt.edu.cn)

This work was supported in part by the National Natural Science Foundation of China under Grant 61574081, Grant 61504065, and Grant 61704084, and in part by the Graduate Students Research Innovation Program of Jiangsu Province under Grant 46888ZZ16255.

**ABSTRACT** The drift region shape factor ( $L_d/t$ ) plays a sophisticated role in affecting reduced surface field (RESURF) effect and breakdown characteristics. In this paper, based on the effective doping concentration (EDC) theory, an Improved EDC concept is proposed to explore the impact of shape factor on 2-D coupling effect in RESURF lateral power devices. The Improved EDC concept indicates that the sophisticated 2-D coupling in N-well resulting an effective N-I-P type drift region. Thus, the surface electric field basin may exist because of the expansion of vertical depletion region. The proposed model presents a more adaptive trait in describing 2-D coupling effect under various device structure parameters when compared to the conventional EDC model. Furthermore, a corresponding structure optimization criterion is provided to further improve the tradeoff between breakdown voltage, On-resistance and costs. The results obtained by the proposed model are found to be accurate comparing with TCAD simulation results.

**INDEX TERMS** 1-D model, shape factor, effective doping, RESURF effect, breakdown voltage.

## I. INTRODUCTION

The introduction of Reduced Surface Field (RESURF) technique enables lateral power devices to operate one-step closer to the ideal switch that features infinite electrical conductivity or resistivity when turned ON or OFF [1]–[8]. It has been widely accepted in lateral power design that a good tradeoff between BV and Ron can be achieved when doping dose ( $Q = N_d \times t_s$ ) fulfills RESURF principle. However, except the epitaxial layer thickness ( $t_s$ ), the breakdown characteristic is also a strong function of drift region length ( $L_d$ ) [5], [9]–[11]. Also, the drift region length has a great impact on the Ron. More importantly, the device area is closely related to the costs while the lateral approach is more area-consumable than vertical solutions [1], [3]. In order to be commercially competitive, it is vital for a lateral power device to achieve a good device area utilization rate. In practical, a long drift region may result in a surface

electric field basin [5]–[8]. The existence of this electric field basin indicates that there is one part of drift region contributes to neither lateral nor vertical breakdown voltage. Whereas, the electric field basin doesn't exist when the drift region is short enough. Apparently, the variation of the drift region shape factor alters the 2-D coupling effect between the vertical and lateral structure [12]–[14]. Hence, a reasonable inference can be drawn that the drift region shape factor ( $L_d/t$ ) ought to be considered in designing to achieve a good performance and low costs.

In order to take the benefits of both the simplicity of 1-D models and the veracity of 2-D models, the EDC model has been proposed to provide reasonable physical insight for the 2-D coupling effect [7]. Though EDC models are proven to be sufficiently simple and accurate in describing surface electric field profile and breakdown mechanism at short drift region cases, with the increase of  $L_d$ , abnormal

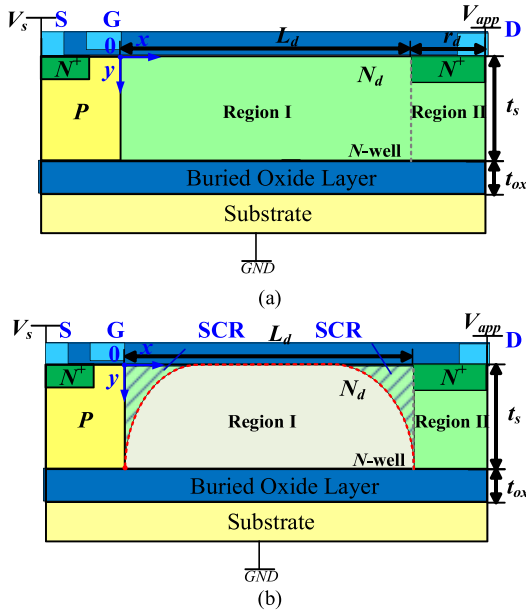


**FIGURE 1.** 2-D cross section of (a) the SOI RESURF LDMOS and (b) the Improved EDC equivalent structure for modeling ( $x - y$  plane).

deteriorations in accuracy are observed [3], [7], [14]. It has been clear that the rectangle Sharing Charge Region (SCR) assumption is too simple to enable conventional EDC model depicts the complexity of Vertical Depletion Region (VDR) expansion when  $L_d/t \gg 2$ . Even the 2-D models consider the breakdown structure as a rectangle region for modeling to reduce its complexity.

In this paper, in order to enrich the EDC theory and provide a universal optimization criterion, we propose an improved EDC concept to explore the impact of Shape factor-induced 2-D coupling effect on BV characteristics. The improved EDC concept indicates that the excessively long drift region enhances the vertical depletion and thus creating a surface electric field basin which provides no benefits to device's BV characteristic. To our knowledge, the improved EDC theory and corresponding 1-D model is the first methodology that can qualitatively and quantitatively explore the influence of shape factor on RESURF effect. The analytical model is validated by the good agreement between the modeling results and simulation results by MEDICI, a commercial TCAD tool. The simulation models used in MEDICI are CONSRH, AUGER, BGN, FLDMOB, IMPACT.I and CCSMOB.

## II. EFFECTIVE DOPING CONCENTRATION

For the 2-D cross-section shown in Fig. 1(a), when a reverse-biased voltage is applied, the potential function in the silicon film satisfies the 2-D Poisson's equation, which yields:

$$\frac{\partial^2 \varphi(x, y)}{\partial x^2} + \frac{\partial^2 \varphi(x, y)}{\partial y^2} = -\frac{qN_d}{\epsilon_s} \quad (1)$$

By using the second-order Taylor series expansion along the  $y$  dimension, a general differential equation for the surface

potential distribution function can be given by:

$$\frac{\partial^2 \varphi(x, 0)}{\partial x^2} - \frac{\varphi(x, 0)}{t^2} = -\frac{qN_d}{\epsilon_s} \quad (2)$$

The EDC theory assumes that the impact of 2-D/3-D effect on BV characteristic can be equivalent to the variation of EDC profile of drift region. When the device operates in off state, a Sharing Charge Region (SCR) is formed to sustain applied reverse voltage. The SCR is limited by the lateral and vertical depletion length  $x_{lat}$  and  $x_{ver}(x)$ , respectively. In conventional EDC model, as shown in Fig. 1(a), such an SCR is considered as a rectangle region. Thus, in [3], the EDC profile that contributes to the lateral depletion can be presented with a linear function, which yields:

$$N_{eff}(x) = N_d \left( 1 - \eta \frac{x}{\text{Min}[x_{lat}, L_d]} \right) \quad (3)$$

where  $\eta = x_{ver}(L_d + r_d)/t_s$  is the ratio of the spreading of the VDR into the epitaxial layer under drain region and SOI layer thickness.  $\eta$  also indicates the 2-D coupling effect between lateral structure and Region II. By applying the EDC theory reported in [7], Eq. (2) can be further simplified as:

$$\frac{d^2 \varphi_i(x, 0)}{dx^2} = \frac{dE_i(x, 0)}{dx} = -\frac{qN_{eff}(x)}{\epsilon_s} \quad (4)$$

So far, by using Eq. (3) and (4), the conventional EDC model can be obtained accordingly. Although the conventional EDC model can accurately depict the 2-D coupling effect at short  $L_d$  case, its accuracy drops significantly with the increase of drift region shape factor. In fact, as Fig. 1(a) shows, for a practical lateral power device, the Region I and II together compose the drift region. Apparently, both Region I and II contribute to the 2-D coupling effect. Among them, the vertical depletion region in Region I is limited by the surface electric potential  $\varphi(x, 0)$ . Therefore, the 2-D coupling between Region I and lateral structure highly depends on drift region shape factor. To quantitatively depict the influence of such a 2-D coupling on lateral surface electric potential and field profiles, we propose that only a part of the drift region is involved in lateral depletion and the corresponding EDC can be given as:

$$N_I(x) = N_d \left[ \left( \frac{x}{L_d} \right)^a + \left( 1 - \frac{x}{L_d} \right)^a \right] \quad (5)$$

where  $a = L_d/t$  being the drift region shape factor.  $t = (0.5t_s^2 + Kt_s t_{ox})^{0.5}$  is the characteristic thickness [3],  $K = \epsilon_s/\epsilon_{ox} \approx 3$  is the dielectric constant ratio of silicon and silicon dioxide material,  $t_s$  being the epitaxial layer thickness and  $t_{ox}$  represents the thickness of the buried oxide layer. As shown in Fig. 1(b), Eq. (5) indicates that the parts of drift region away from  $\text{PN}_d$  and  $\text{N}^+\text{N}_d$  junctions tend to have less contribution to the 2-D coupling effect. Accordingly, by considering the 2-D coupling effect in Region I, Eq. (3) is replaced by:

$$N_{eff}(x) = N_I(x) \left( 1 - \eta \frac{x}{\text{Min}[x_{lat}, L_d]} \right) \quad (6)$$

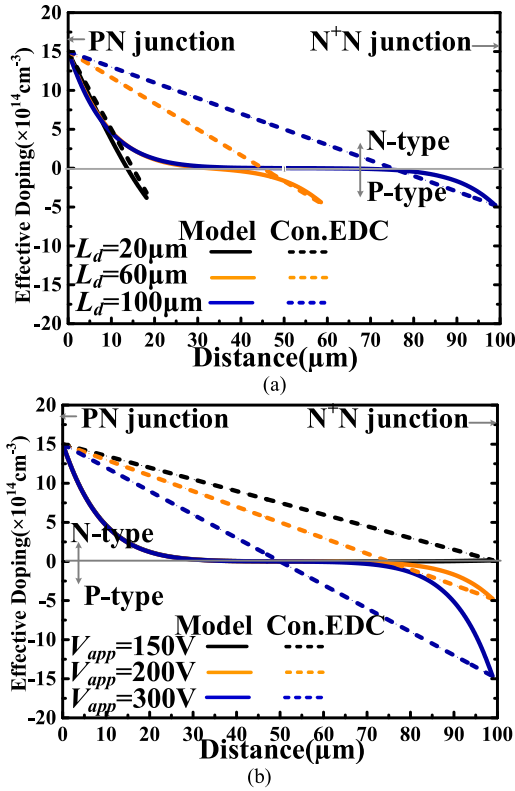


**FIGURE 2.** Drift region Effective Doping Concentration of the drift region for various (a). drift region length ( $V_{app} = 200\text{V}$ ,  $N_d = 1.5 \times 10^{15}\text{cm}^{-3}$ ,  $t_s = 7\mu\text{m}$ ), (b). applied voltage ( $N_d = 1.5 \times 10^{15}\text{cm}^{-3}$ ,  $t_s = 7\mu\text{m}$ ,  $L_d = 100\mu\text{m}$ ) with  $t_{ox} = 2\mu\text{m}$ .

It is worthy to be noted that the EDC profile obtained by Eq. (6) can also be applied to explore the 2-D coupling effect in bulk silicon case. To do so, the characteristic thickness ought to be amended to  $t = (0.5t_s^2 + t_s t_{sub})^{0.5}$ .

Fig. 2 intuitively illustrate the variation of EDC profile under various structure parameters and bias. As shown in Fig. 2(a), when shape factor is relatively small, the proposed EDC profile tends to coincide with the conventional EDC profile defined by Eq. (3). For a fixed vertical structure, the increase of drift region length results in a deviation of EDC from linear estimation. As shown in Fig. 2(a) and (b), although the  $N_{eff}(0)$  and  $N_{eff}(L_d)$  that obtained by Eq. (3) and (6) are same, the difference of EDC within the drift region indicates the SCR is overestimated by the conventional EDC model. As illustrated in Fig. 2(b), an equivalent intrinsic region appears in the drift region which means no charges in this region contributes to the lateral depletion. Such an equivalent intrinsic region forms an equivalent N-I-P drift region. Therefore, as shown in Fig. 3, a surface electric field basin may be expected under long drift region cases. In its essence, an excessively long drift region weaken the grip of lateral  $\text{PN}_d$  and  $\text{N}^+\text{N}_d$  junctions on drift region. The charges that far away from the source and drain region is more easily being affected by vertical structure and thus forming a hump-shaped VDR shown in Fig. 1(b).

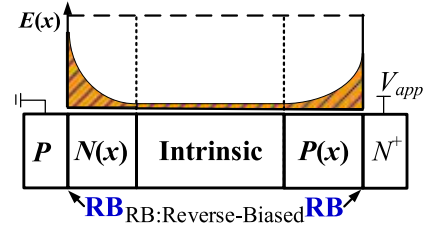


**FIGURE 3.** Effective NIP-type lateral structure and the electric field distribution of the RESURF lateral power device.

### III. VERIFICATION AND DISCUSSION

#### A. SURFACE ELECTRIC FIELD PROFILE

As the 2-D coupling effect on the lateral structure is reflected by EDC that Eq. (6) defines, the surface electric field (EF) profile  $E(x,0)$  can be obtained by submitting Eq. (6) to 1-D Poisson's function [Eq. (4)], which yields:

$$E(x,0) = E_0 - \frac{qN_d L_d}{(a+1)\epsilon_s} \left[ (1-\eta) \left(\frac{x}{L_d}\right)^{a+1} - \left(1 - \frac{x}{L_d}\right)^{a+1} + 1 \right] \quad (7)$$

The Eq. (7) can be further simplified without causing the observable error when  $a > 5$ , which yields:

$$E(x,0) = E_0 - \frac{qN_d L_d}{a\epsilon_s} \left[ (1-\eta) \left(\frac{x}{L_d}\right)^a - \left(1 - \frac{x}{L_d}\right)^a + 1 \right] \quad (8)$$

According to Eq. (8), when drift region shape factor satisfies  $a = 1$ , the proposed model is consistent with conventional EDC model. To further validate the correctness of proposed methodology, we have compared the modeled surface electric field with results obtained by TCAD and conventional EDC model in Fig. 4. As shown in Fig. 4(a) and (b), when shape factor is relatively small ( $L_d/t \approx 2$ ), the conventional EDC model is capable maintain a good consistency between simulation results. Whereas, as the shape factor increases with the lengthening of drift region, the rectangle SCR assumption resulting in a large mismatch in EF profile with simulations can be observed. Meanwhile, as the improved EDC model simultaneously considers both the 2-D coupling effect of Region I and II, such mismatch is no longer exist. Furthermore, as shown in Fig. 4(b)-(d), since the bump-shaped VDR in Region I only determined by drift region shape factor, the variation of applied voltage has no effect on the equivalent intrinsic region. In other words, the surface electric field basin is inevitable for an excessively long drift region.

Notably, same as that in conventional EDC model, the surface EF peaks at  $\text{PN}_d$  and  $\text{N}^+\text{N}_d$  junctions reach the same height when  $\eta = 2$ . In which case, the maximum lateral breakdown voltage is achieved as lateral EF peaks reach critical electric field ( $E_C$ ) simultaneously [7].

#### B. BREAKDOWN VOLTAGE

For a lateral power device, the lateral and vertical structures simultaneously sustain reversed-biased voltage. The

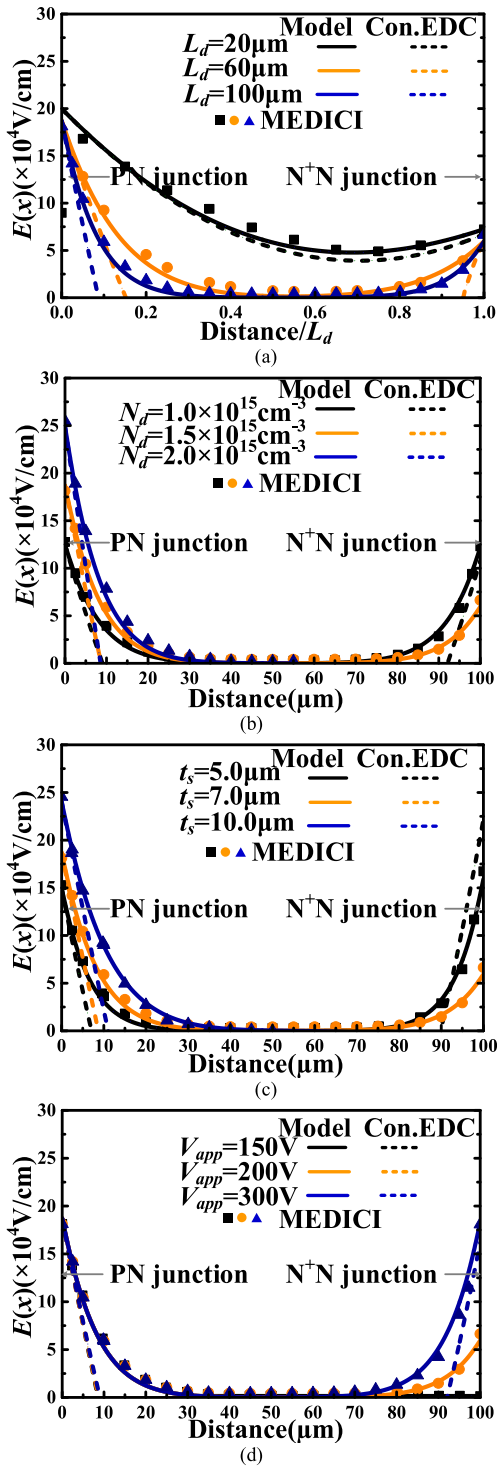


**FIGURE 4.** Analytical and numerical surface electric field profiles of the drift region for various (a). drift region length ( $V_{app} = 200V$ ,  $N_d = 1.5 \times 10^{15} \text{ cm}^{-3}$ ,  $t_s = 7 \mu\text{m}$ ), (b). drift region doping ( $V_{app} = 200V$ ,  $t_s = 7 \mu\text{m}$ ,  $L_d = 100 \mu\text{m}$ ), (c). epitaxial layer thickness ( $V_{app} = 200V$ ,  $N_d = 1.5 \times 10^{15} \text{ cm}^{-3}$ ,  $L_d = 60 \mu\text{m}$ ) and (d). applied voltage ( $N_d = 1.5 \times 10^{15} \text{ cm}^{-3}$ ,  $t_s = 7 \mu\text{m}$ ,  $L_d = 100 \mu\text{m}$ ) with  $t_{ox} = 2 \mu\text{m}$ .

BV of the device is limited by the minimum of lateral and vertical BV. In full-depletion condition, the RB voltage that lateral structure sustains can be given by using

Eq. (4) and (7):

$$V_{lat} = E_0 L_d - (a + 2 - \eta) V_0 \left[ \frac{a^2}{(a + 1)(a + 2)} \right] \quad (9)$$

where  $V_0 = qN_d t^2 / \epsilon_s$ ,  $E_0$  is the surface electric field at  $x = 0$ . Same as the EDC model, the proposed EDC methodology can also be applied to elaborate the partially depleted. Nevertheless, the partially depleted breakdown is a lack of meaning in the application of lateral power devices, we will not elaborate it in this paper. As shown in Fig. 3 and 4, the lateral structure has two electric field peaks at the two ends of the drift region, respectively. Therefore, for the full-depletion lateral breakdown, there are two cases. For  $\text{PN}_d$  junction breakdown case ( $\eta < 2$ ),  $E_C = E_0$ . Whereas, for the  $\text{N}^+\text{N}_d$  breakdown case ( $\eta = 2$ ),  $E_C = E(L_d, 0)$ . Hence the lateral BV can be obtained as:

$$BV_{lat} = \begin{cases} E_C L_d - (a + 2 - \eta) V_E, & \eta < 2 \\ E_C L_d - [(a + 1)\eta - a - 2] V_E, & \eta \geq 2 \end{cases} \quad (10)$$

where  $E_C = 3.0 \times 10^5 / [1 - 0.33 \log_{10}(N_d / 10^{16})] (\text{V/cm})$  [3], [4], [7], [13], [14] is the critical electric field,  $V_E = V_0 [a^2 / (a^2 + 3a + 2)]$ . Apparently, as discussed above, the lateral breakdown voltage reaches its maximum ( $BV_{lat\_Max}$ ) when  $\eta = 2$ . For a high shape factor case ( $a > 5$ ), the Eq. (10) can be further simplified while maintaining its accuracy, which yields:

$$BV_{lat} = \begin{cases} E_C L_d - (a + 2 - \eta) V_0, & \eta < 2 \\ E_C L_d - [(a + 1)\eta - a - 2] V_0, & \eta \geq 2 \end{cases} \quad (11)$$

As for the vertical breakdown voltage, its mathematical expression can be given by:

$$BV_{ver} = \frac{qN_d t_s}{\epsilon_s} \left( K\eta t_{ox} + \frac{2\eta - 1}{2} t_s \right) \quad (12)$$

The device breakdown voltage is determined by the lowest breakdown voltage among lateral and vertical structures, which yields:

$$BV = \text{Min} [BV_{lat}, BV_{ver}] \quad (13)$$

Fig. 5(a) and (b) show the  $BV - N_d$  and  $BV - L_d$  characteristics. As shown Fig. 5(a), with the increase of drift region doping concentration, the breakdown of lateral power device successively undergoes four stages:  $\text{N}^+\text{N}_d$  junction full depletion ( $BV_{lat}^{\text{FNN}}$ ), vertical breakdown ( $BV_{ver}$ ),  $\text{PN}_d$  junction full depletion ( $BV_{lat}^{\text{FPN}}$ ) and  $\text{PN}_d$  junction partial depletion ( $BV_{lat}^{\text{PPN}}$ ). In order to achieve a high breakdown voltage while maintaining an acceptable process tolerance, in practical, lateral power devices are designed to have the vertical breakdown when the critical electric field is reached. As Fig. 5(a) intuitively shows, a longer drift region length means a bigger process tolerance. However, a longer  $L_d$  also results in bigger  $R_{on}$  and lower area utilization rate. Considering the fact that the  $N_d$  is normally varying between  $0.9\text{--}1.1N_d$  in fabrication, an excessively long drift region is not only unnecessary but also uneconomic. For example, when the designed optimized  $N_d = 1.65 \times 10^{15} \text{ cm}^{-3}$ ,



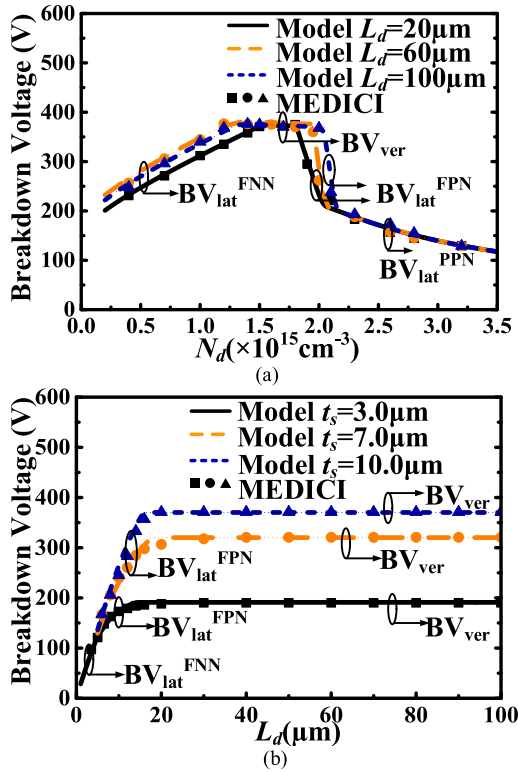


**FIGURE 5.** The dependence of breakdown voltage on (a). drift region doping ( $t_s = 7 \mu\text{m}$ ) and (b). drift region length ( $N_d = 1.5 \times 10^{15} \text{ cm}^{-3}$ ) with  $t_{ox} = 2 \mu\text{m}$ .

the variation of  $N_d$  is within  $1.5\text{--}1.8 \times 10^{15} \text{ cm}^{-3}$ . Therefore, as Fig. 5(a) indicates, when  $L_d = 20 \mu\text{m}$ , the process tolerance constraint has already been met. Meanwhile, a longer drift region would inevitably result in a higher Ron and larger device area. As shown in Fig. 5(b), with the increase of  $L_d$ , the breakdown of lateral power device successively undergoes three stages:  $N^+N_d$  junction full depletion ( $BV_{lat}^{FNN}$ ),  $PN_d$  junction full depletion ( $BV_{lat}^{FPN}$ ) and vertical breakdown ( $BV_{ver}$ ). The vertical breakdown occurs when  $BV_{lat\_Max} > BV_{ver}$ . After reaching the vertical breakdown, the increase of drift region length will no longer increase the BV. In such case, the BV is limited by Eq. (12). By using Eq. (12) and (10), to achieve the vertical breakdown voltage, the drift region length requirement yields as follows:

$$L_d > (8t^2 - 3t_s^2) / (8t_s - 4t) \quad (14)$$

As shown in Fig. 4(a), an electric field basin exists in long drift region cases which means the drift region is only partially contributing to lateral depletion resulting in a low area utilization. In this paper, an Area Utilization Rate (AUR) is defined as  $AUR = BV_{lat\_MAX} / (E_C L_d)$  to evaluate the surface area utilization in drift region designing. For an ideal case, the surface electric field reaches even, thus the  $AUR = 1$ . For a RESURF lateral power device, the maximum AUR can be obtained by using  $\eta = 2$  and Eq. (10),

which yields:

$$AUR = 1 - \frac{V_0}{E_C t} \frac{a^2}{a^2 + 3a + 2} \quad (15)$$

As Eq. (15) indicates, the AUR is not a linear function of  $L_d$ . For the devices shown in Fig. 4(a), since  $L_d = 20 \mu\text{m}$  already satisfies Eq. (14), the AUR can be improved more than 11% when drift region length shrunk from 100 to  $20 \mu\text{m}$  while maintaining the same device BV.

So far, by using the improved EDC model, the surface electric field profile and breakdown voltage have been qualitatively and quantitatively discussed. As shown in Fig. 4 and 5, the consistency between the analytical solution and the simulation has demonstrated the proposed EDC to be valid. It worthy to be noted that, by submitting Eq. (6), (8) and (11), it can be found that the proposed model also consistent with 2-D Poisson function, thus further verifying the efficiency of the proposed methodology.

#### IV. STRUCTURE OPTIMIZATION

For a lateral power device, the goal of structure optimization is to achieve a good tradeoff between the BV, Ron, and area utilization. Due to a complicated role that shape factor plays in affecting On/Off characteristics and area utilization, it is essential to optimize the geometric structure of drift region during the design phase. Considering the shape factor-induced 2-D coupling, such a complicated 2-D effect also leads to a higher degree of optimization complexity. Clearly, the conventional RESURF criterions are too simple to provide effective designing guidance.

As discussed above, in order to maintain a high BV while achieving a big process tolerance, it is desirable to make device happens vertical breakdown. Accordingly, the theoretical window for optimizing the drift region doping dose ( $Q = N_d \times t_s$ ) can be obtained by using Eq. (10) and (12). The upper ( $Q_{up}$ ) and lower ( $Q_{down}$ ) limits of the optimized doping dose (ODD) can be given as:

$$Q_{up} = \frac{\epsilon_s E_C}{q} \left[ \frac{2 + b^2 - 2ab - 2a^2 / (a^2 + 3a + 2)}{1 - 2a^2 / (a + 1)} \right] \quad (16)$$

$$Q_{down} = \frac{\epsilon_s E_C}{q} \left[ \frac{2 + b^2 - 2ab + 2a^2 / (a + 2)}{1 + 2a^2 / (a + 1)} \right] \quad (17)$$

where  $b = t_s/t$  is the vertical structure factor. For the simplicity, the  $E_C$  used in Eq. (16) and (17) is  $E_C = 3.0 \times 10^5 \text{ (V/cm)}$  [7], [14]. Hereby, the structure optimization criterion can be given as:

$$Q_{down} \leq Q \leq Q_{up} \quad (18)$$

As discussed above, to realize vertical breakdown, for a fixed vertical structure, the drift region length has to exceed the length requirement limited by Eq. (14). However, a longer drift region also means a smaller area utilization rate. Thus, as shown in Fig. 6(a), when the drift region length satisfies  $L_d > 5t$ , the shape factor has a small impact on the drift

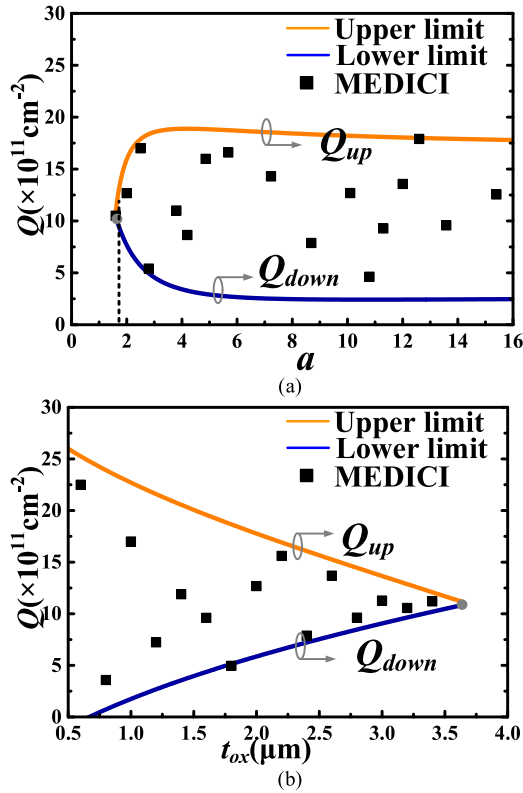


**FIGURE 6.** Drift region doping dose as a function of (a). shape factor ( $t_{ox} = 2\mu\text{m}$ ) and (b). BOX layer thickness with  $t_s = 3\mu\text{m}$ .

region ODD. In such case, Eq. (16) and (17) can be further simplified as:

$$Q_{up} = \frac{\epsilon_s E_C}{q} \left( \frac{2 + b^2 - 2ab - 2}{1 - 2a} \right) \quad (19)$$

$$Q_{down} = \frac{\epsilon_s E_C}{q} \left( \frac{2 + b^2 - 2ab + 2a}{1 + 2a} \right) \quad (20)$$

In order to verify the proposed EDC model and optimization method, we simulate the BV and EF profile under two drift region length. As shown in Fig. 7, when the vertical structure of the lateral power device is fixed as  $t_{ox} = 2\mu\text{m}$ ,  $t_s = 7\mu\text{m}$ , the characteristic thickness  $t$  is about  $8.2\mu\text{m}$ . For the long drift region case, as shown in Fig. 7(a), the shape factor  $a = L_d/t$  is about 7.32 ( $L_d = 60\mu\text{m}$ ). According to Eq. (16) and (17),  $Q = 11.0 \times 10^{11} \text{ cm}^{-2}$  ( $N_{d,opt} = 1.6 \times 10^{15} \text{ cm}^{-3}$ ) satisfies the ODD. Meanwhile, for a short drift region case, as shown in Fig. 7(b)-(c), the drift region length is  $20\mu\text{m}$ , thus the shape factor is about 2.44. Considering the maximum process tolerance ( $\pm 10\% N_{d,opt}$ ), the  $N_d$  used in the devices shown in Fig. 7(b) and (c) are  $1.45$  and  $1.85 \times 10^{15} \text{ cm}^{-3}$ , respectively. As shown in Fig. 7(a)-(c), for a fully depleted drift region, three electric occur at: 1) the PN junction (A-Point); 2)  $N^+N$  junction (B-Point) and 3) Si-SiO<sub>2</sub> interface under the drain region (C-Point). As shown in Fig. 7(d), the simulation results indicate that both long and short drift region cases reach the vertical breakdown at  $BV=325\text{V}$  simultaneously. Therefore,

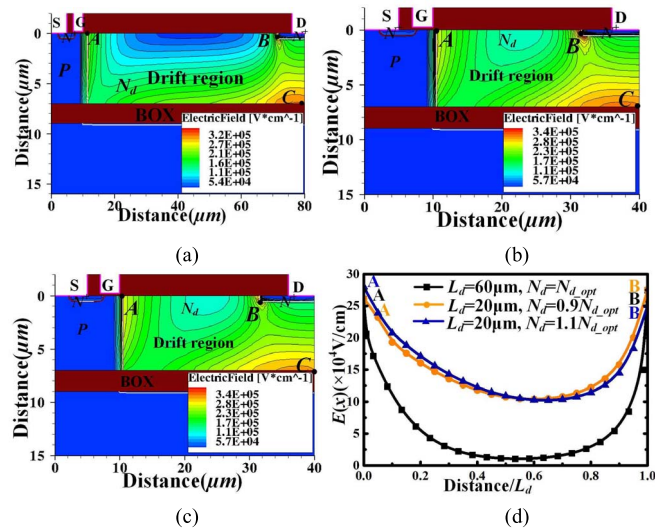


**FIGURE 7.** Distribution of potential contours at  $BV = 325 \text{ V}$  of (a). long drift region case ( $L_d = 60\mu\text{m}$ ), (b). short drift region case with  $N_d = 0.9N_{d,opt}$ , (c). short drift region case with  $N_d = 1.1N_{d,opt}$  and comparison of (d) surface electric field profile under an unified coordinate.

even the drift region length shrinks by 67%, the same BV characteristic can still be achieved. Moreover, when the drift region length decreases from  $60$  to  $20\mu\text{m}$ , the BFOM improves 8 times. In light of that, the proposed optimization method can be considered as an effective tool in optimizing RESURF lateral power device on SOI substrate. As shown in Figs. 6 and 7, the predictions of the proposed EDC model agree very well with the TCAD simulation.

## V. CONCLUSION

In order to enrich the conventional EDC model and elaborate the physical meaning of the shape factor-induced 2-D coupling effect, we proposed the improved EDC concept. The proposed EDC concept indicates that for a long drift region case the drift region can be equivalent as a 1-D N-I-P structure. Therefore, as a result of the expansion of the VDR, a surface electric field basin may occur when the drift region is long enough. Using the improved EDC concept, a novel 1-D analytical model is proposed to qualitatively and quantitatively explore the impact of shape factor-induced 2-D coupling on surface electric field and breakdown characteristics for the first time. Based on the proposed EDC concept, an effective optimization criterion is proposed to provide designing guidance. The analytical solutions are found out to be consistent with TCAD simulations.

## REFERENCES

- [1] D. Disney, T. Letavic, T. Trajkovic, T. Terashima, and A. Nakagawa, "High-voltage integrated circuits: History, state of the art, and future prospects," *IEEE Trans. Electron Devices*, vol. 64, no. 3, pp. 659–673, Mar. 2017, doi: [10.1109/TEDE.2016.2631125](https://doi.org/10.1109/TEDE.2016.2631125).
- [2] X. Luo *et al.*, "Ultralow ON-resistance high-voltage P-channel LDMOS with an accumulation-effect extended gate," *IEEE Trans. Electron Devices*, vol. 63, no. 6, pp. 2614–2619, Jun. 2016, doi: [10.1109/TEDE.2016.2555327](https://doi.org/10.1109/TEDE.2016.2555327).

- [3] J. Zhang *et al.*, "A new physical insight for the 3-D-layout-induced cylindrical breakdown in lateral power devices on SOI substrate," *IEEE Trans. Electron Devices*, vol. 65, no. 5, pp. 1843–1848, May 2018, doi: [10.1109/TEDE.2018.2810325](https://doi.org/10.1109/TEDE.2018.2810325).
- [4] M. Imam, M. Quddus, J. Adams, and Z. Hossain, "Efficacy of charge sharing in reshaping the surface electric field in high-voltage lateral RESURF devices," *IEEE Trans. Electron Devices*, vol. 51, no. 1, pp. 141–148, Jan. 2004, doi: [10.1109/TEDE.2003.821383](https://doi.org/10.1109/TEDE.2003.821383).
- [5] S.-K. Chung, S.-Y. Han, J.-C. Shin, Y.-I. Choi, and S.-B. Kim, "An analytical model for minimum drift region length of SOI RESURF diodes," *IEEE Electron Devices Lett.*, vol. 17, no. 1, pp. 22–24, Jan. 1996, doi: [10.1109/55.475565](https://doi.org/10.1109/55.475565).
- [6] A. Ferrara *et al.*, "Ideal RESURF geometries," *IEEE Trans. Electron Devices*, vol. 62, no. 10, pp. 3341–3347, Oct. 2015, doi: [10.1109/TEDE.2015.2460112](https://doi.org/10.1109/TEDE.2015.2460112).
- [7] Z. Jun *et al.*, "One-dimensional breakdown voltage model of SOI RESURF lateral power device based on lateral linearly graded approximation," *Chin. Phys. B*, vol. 24, no. 2, 2015, Art. no. 028502, doi: [10.1088/1674-1056/24/2/028502](https://doi.org/10.1088/1674-1056/24/2/028502).
- [8] J. A. Appels and H. M. J. Vaes, "High voltage thin layer devices (RESURF devices)," in *Proc. Int. Electron Devices Meeting*, 1979, pp. 238–241, doi: [10.1109/IEDM.1979.189589](https://doi.org/10.1109/IEDM.1979.189589).
- [9] J. Wei *et al.*, "High-voltage thin-SOI LDMOS with ultralow ON-resistance and even temperature characteristic," *IEEE Trans. Electron Devices*, vol. 63, no. 4, pp. 1637–1643, Apr. 2016, doi: [10.1109/TEDE.2016.2533022](https://doi.org/10.1109/TEDE.2016.2533022).
- [10] I. Cortés *et al.*, "Analysis and optimization of lateral thin-film silicon-on-insulator (SOI) MOSFET transistors," *Microelectron. Rel.*, vol. 52, no. 3, pp. 503–508, 2012, doi: [10.1016/j.microrel.2011.12.011](https://doi.org/10.1016/j.microrel.2011.12.011).
- [11] X. She, A. Q. Huang, Ó. Lucía, and B. Ozpineci "Review of silicon carbide power devices and their applications," *IEEE Trans. Ind. Electron.*, vol. 64, no. 10, pp. 8193–8205, Oct. 2017, doi: [10.1109/TIE.2017.2652401](https://doi.org/10.1109/TIE.2017.2652401).
- [12] F. Udrea, G. Deboy, and T. Fujihira, "Superjunction power devices, history, development, and future prospects," *IEEE Trans. Electron Devices*, vol. 64, no. 3, pp. 713–727, Mar. 2017, doi: [10.1109/TEDE.2017.2658344](https://doi.org/10.1109/TEDE.2017.2658344).
- [13] Y. Guo, J. Yao, B. Zhang, H. Lin, and C. C. Zhang, "Variation of lateral width technique in SOI high-voltage lateral double-diffused metal-Oxide-Semiconductor transistors using high-K dielectric," *IEEE Electron Device Lett.*, vol. 36, no. 3, pp. 262–264, Mar. 2015, doi: [10.1109/LED.2015.2393913](https://doi.org/10.1109/LED.2015.2393913).
- [14] J. Zhang *et al.*, "Effective doping concentration theory: A new physical insight for the double-RESURF lateral power devices on SOI substrate," *IEEE Trans. Electron Devices*, vol. 65, no. 2, pp. 648–654, Feb. 2018, doi: [10.1109/TEDE.2017.2786139](https://doi.org/10.1109/TEDE.2017.2786139).



**JUN ZHANG** (M'17) received the B.S. degree in microelectronics from the Nanjing University of Posts and Telecommunications, Nanjing, China, in 2013, where he is currently pursuing the Ph.D. degree in microelectronics and solid-state electronics under the supervision of Prof. Y. Guo. He has been a Visiting Scholar with the University of Texas at Austin since 2016. His current research interests include semiconductor power devices, microelectronics devices reliability, and RF and power integrated circuits and systems.



**YUFENG GUO** (M'05) received the B.Eng. and M.Eng. degrees in material science and engineering from Sichuan University, Chengdu, China, in 1996 and 2001, respectively, and the Ph.D. degree in microelectronics and solid-state electronics from the University of Electronic Science and Technology of China, Chengdu, China, in 2005. He served as a Lecture from 2005 to 2007, an Associate Professor from 2007 to 2012, and has been a Professor since 2012 with the Nanjing University of Posts and Telecommunications,

Nanjing, China, where he is currently the Dean of the College of Electronic and Optical Engineering and the Vice-Director of National and Local Joint Engineering Laboratory of RF Integration and Micro-Assembly Technology. He has published over 180 articles in refereed journals and conferences and holding over 20 Chinese patents.



**DAVID Z. PAN** (S'97–M'00–SM'06–F'14) is currently a Engineering Foundation Professor with the University of Texas at Austin. His research interests include cross-layer IC design for manufacturability, reliability, security, physical design, analog design automation, and CAD for emerging technologies. He has published over 280 refereed technical papers and holds 8 U.S. patents. He has graduated over 20 Ph.D. students who are now holding key academic and industry positions. He has served as a Senior Associate Editor for *ACM Transactions on Design Automation of Electronic Systems*, and an Associate Editor for a number of other journals.